Atmospheric Pressure Plasma Surface Modification of Poly(D,L-lactic acid) Increases Fibroblast, Osteoblast and Keratinocyte Adhesion and Proliferation

Filippo Renò,* Domenico D'Angelo, Gloria Gottardi, Manuela Rizzi, Davide Aragno, Giacomo Piacenza, Federico Cartasegna, Miriam Biasizzo, Francesco Trotta, Mario Cannas

An atmospheric pressure plasma deposition for P(d,L)LA (PLA) film was used to modify polymer surface properties using 1,2-diaminopropane and acrylic acid as precursors. These two different plasma coatings result in a high density of amino groups (PLA-NH_2) and carboxylic groups (PLA-COOH) onto PLA surface as demonstrated by Fourier transform infra-red (FTIR) spectroscopy and X-ray photoelectron spectroscopy (XPS). Plasma coatings modified PLA surface wettability and proteins adsorption from fetal bovine serum (FBS), influencing cell adhesion and proliferation of 3T3 mouse fibroblast, MC-3T3 E1 mouse pre-osteoblast, and HaCaT cells (human keratinocytes). In particular both coatings increased pre-osteoblast and keratinocyte adhesion while no effect was observed on fibroblast. Moreover, cell proliferation assessed after 48 h by Tox-8 assay was significantly higher for osteoblast cells and keratinocyte seeded onto both PLA-NH_2 and PLA-COOH compared to cells seeded onto normal PLA. On the basis of the obtained data, the atmospheric pressure plasma deposition described might represent an innovative and useful tool for bone and skin tissue engineering.

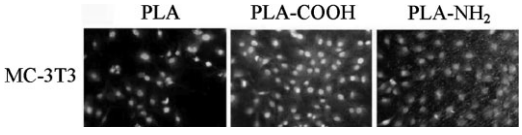

1. Introduction

Polylactic acid is a biodegradable aliphatic polymer existing both as P(L)LA and P(D,L)LA (hereafter PLA). PLA undergoes scission in the body to lactic acid with L-lactic acid as a natural intermediate in carbohydrate metabolism.[1,2]

Thus PLA is suitable for use in reabsorbable sutures, carriers for drug and growth factors delivery, peripheral

Prof. F. Renò
Clinical and Experimental Medicine Department, University of Eastern Piedmont "A.Avogadro", Via Solaroli 17, 28100 Novara, Italy
E-mail: filippo.reno@med.unipmn.it
Prof. F. Renò, M. Rizzi, D. Aragno, M. Cannas
Research Centre for Biomaterials and Tissue Engineering, Clinical and Experimental Medicine Department, University of Eastern Piedmont "A. Avogadro", Via Solaroli 17, 28100 Novara, Italy

D. D'Angelo, G. Piacenza, F. Cartasegna
Clean NT Lab division, Environment Park S.p.A., Via Livorno 60, 10144 Turin, Italy
G. Gottardi
Fondazione Bruno Kessler, Plasma, Advanced Materials and Surface Engineering Research Unit, Centre for Materials and Microsystems, via Sommarive 18, 38123 Povo (Trento), Italy
M. Biasizzo, F. Trotta
Chemistry Department I.F.M., University of Turin, Via Pietro Giuria 7, 10125 Turin, Italy

DOI: 10.1002/ppap.201100139

nerve guidance channels, vascular devices, and implants for orthopedic surgery also thanks to its good mechanical property system.[3,4]

However, the hydrophobicity and low surface energy of these polymers lead to inefficient cell attachment, spreading, and proliferation.[5] Biologic response to biomaterials implantation is determined by their surface characteristics rather than bulk properties, therefore a wide range of surface modification methodologies have been used to modify their surface chemistry, wettability, surface energy, and topography in order to modulate cellular responses such as cell adhesion or foreign body reaction.[6–9] The optimal surface modification technique should be able to induce physical and/or chemical modifications of the outer molecular layer of the biomaterial surface, without affecting the bulk properties of the material (e.g., mechanical resistance or degradation kinetics).[6] In the last few years gas plasma treatments have been widely used for the production of modified biomaterials for tissue engineering.[10]

Plasma surface activation employs gases, such as oxygen or argon, which dissociate and react with the surface, creating additional functional groups that can be recognized as adhesion sites for surrounding cells,[11–13] whereas N_2 and NH_3 treatments incorporate both nitrogen and oxygen containing groups depending on whether the treated surface is subsequently exposed to air.[14,15] Plasma grafting (obtained by plasma treatment with gases) is distinct from plasma polymerization because the first grafts functional groups on the polymer surface while the second one coats the substrate with covalently bind thin film. Two of the most common monomers used for plasma polymerization in vacuum on biodegradable polymers are 1,2-diaminopropane (DAP) and acrylic acid (AA).[16,17]

Polylactide polymers do not contain functional groups such as carboxyl and hydroxyl groups which enhance cell adhesion by increasing surface hydrophilicity[18] or amino groups that enhance the adhesion of epithelial cells[19] therefore they are optimal candidates for gas plasma surface modifications.[20–23]

In this paper an atmospheric pressure plasma deposition is described to modify PLA films surface properties such as wettability and proteins adsorption, in order to enhance its ability to induce cell adhesion and proliferation. As during plasma polymerization monomers may undergo considerable decomposition or fragmentation of chemical functions, studies of active species into the plasma during the polymerization were performed to obtain information concerning the type of radicals formed and participating in plasma polymerization. In fact free radicals can be formed by three possible steps: (i) opening a double or triple bond, (ii) cleaving a C–C bond, and (iii) by hydrogen abstraction. The contribution of these three steps was investigated by measuring the change of pressure of a closed system and by estimation of hydrogen production. Characterization of the plasma system was performed by optical emission spectroscopy (OES); untreated and treated surfaces were characterized by measuring the surface contact angle and performing Fourier transform infra-red spectroscopy (FTIR) and X-ray photoelectron spectroscopy (XPS) analyses. The adsorption of proteins from fetal bovine serum (FBS) was also studied as a function of gas plasma coating and cell adhesion and proliferation onto PLA and plasma modified PLA samples was assessed using 3T3 mouse fibroblast, MC-3T3 E1 murine pre-osteoblasts, and immortalized human keratinocytes (HaCaT).

2. Experimental Section

2.1. P(D,L)LA Film Preparation

P(D,L)LA (100% D,L, average mol wt 75 000–120 000) was purchased from Sigma–Aldrich (Milwaukee, WI, USA). PLA films were prepared by casting $0.05\,g\cdot ml^{-1}$ PLA solution in chloroform in 150-mm glass dishes. After 5 min shaking the solution was added to glass dishes and the solvent was evaporated at room temperature for 24 h and under vacuum for 3 h in the dark. Transparent film sheets (≈0.5 mm thick) were then cut under sterile conditions into square samples (≈25 cm^2) and stored at 4 °C for no more than 1 week.

2.2. Plasma Deposition

The system employed for plasma coating was based on atmospheric plasma pressure dielectric barrier discharge (APP-DBD Platex 600–Grinp SrL) equipped with a stainless-steel parallel plate electrode of 800 mm × 230 mm × 35 mm size, providing self-plasma impedance adapting glow discharge (Grinp SrL patent[24]). The maximum attainable process power is 2 500 W. A rotary pump and a heating chamber was used to vaporize the precursor. The unit was a lab scale roll to roll version of an industrial production size system and allowed developing dedicated functionalization processes directly scalable up and transferable to industrial production. The configuration of the reactor is shown in Figure 1A,B.

The PLA substrates were always positioned onto a mobile support and very different parameter values was utilized to perform the two different coatings. All the substrates were activated in helium (He) plasma to improve film/substrate interactions through the formation of surface radicals.

Helium gas was used also as a carrier to introduce the different precursors into the plasma region in order to obtain very thin layer of plasma deposited acrylic acid (pdAA) and organic layer containing amino functionalities. In particular, the PLA film samples surfaces were modified by gas plasma at atmospheric pressure using DAP (99% pure, Sigma–Aldrich) to add amino groups (PLA-NH_2) and AA (99% pure, Sigma–Aldrich) to add carboxylic groups (PLA-COOH).

Plasma polymerization of AA was performed treating the substrate for 60 s (three steps of 20 s each) using a power of 60 W

DOI: 10.1002/ppap.201100139

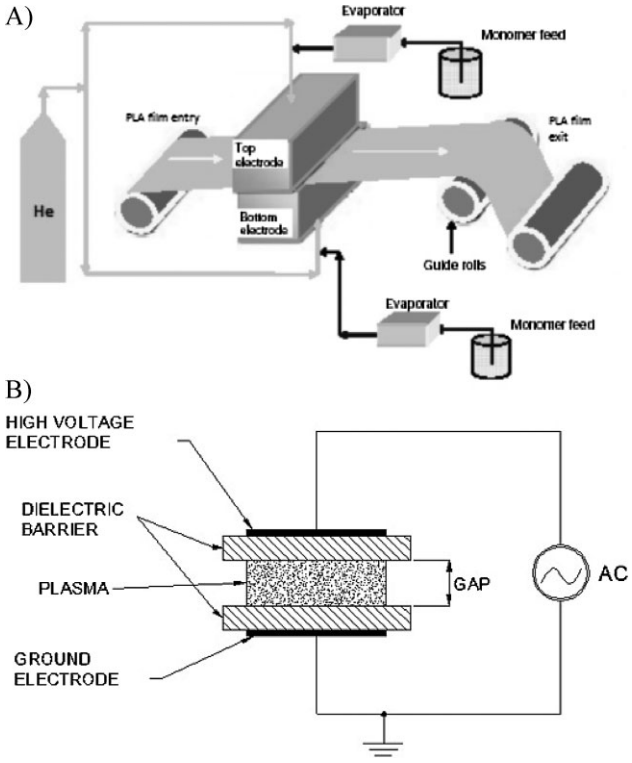

Figure 1. (A) Schematic diagram of atmospheric pressure plasma treatment unit Platex 600 (for courtesy of Grinp S.r.l.). (B) Scheme of the APP-DBD reactor. This system consists of two stainless-steel parallel plate (dimension single Plate 800 mm × 250 mm × 35 mm) electrodes. The power is supply both in continuous and in pulsed mode.

(CW) and 0.26 ml · min^{-1} of AA in order to obtain low monomer fragmentation.

The deposition of organic layer containing amino functionalities was performed, after the described activation, treating the substrate for 60 s (three steps of 20 s each) using a power of 80 W (CW) and 0.20 ml · min^{-1} of DAP.

The effect of the activation in He plasma of the PLA surfaces (hereafter PLA-He) and of the coatings with DAP and AA (hereafter PLA-NH_2 and PLA-COOH, respectively) was checked by XPS and FTIR. Time-related changes on treated surfaces were minimized by testing the samples within the following 48 h.

2.3. Optical Emission Spectroscopy (OES)

Studies of the type of radical present into the plasma have been performed by OES in order to investigate the features of glow-discharge polymerization using an OCEAN Optic Spectrometer.

2.4. Fourier Transformed Infra-red (FTIR) Spectroscopy Analysis

Original and plasma-treated PLA samples were analyzed with FTIR spectroscopy in attenuated total reflection (ATR) mode, using a Perkin Elmer Spectrum 100 instrument. The samples were scanned in the 4 000–650 cm^{-1} region. Each spectrum was recorded with a total of 32 scans and 2.0 cm^{-1} resolution.

2.5. X-ray Photoelectron Spectroscopy (XPS) Analysis

Surface chemical modifications induced by atmospheric plasma coatings were determined by XPS analysis. XPS spectra were recorded with a Scienta-ESCA 200 instrument, equipped with a hemispherical analyzer and a monochromatic Al Kα ($h\nu = 1\,486.6$ eV) X-ray source. The core lines (C1s, O1s, N1s) were acquired at 150 eV pass energy, which leads to an energy resolution of ≈0.4 eV. After a linear-type background subtraction, the spectra were fitted using a non-linear least-squares fitting program adopting a Gaussian–Lorentzian peak shape. Since the samples were exposed to air, the C1s peak included a significant amount of carbon due to environmental contamination. After deconvolution of the C1s core line therefore, the main peak at 285 eV, corresponding to hydrocarbon contamination, was used as internal reference to calibrate the spectra and correct the shift due to charging effects. Compensation of the surface charging was performed by bombarding the surface with an electron flood gun during the analyses.

2.6. Static Water Angle Contact Measurement

Contact angle measurements were carried out in order to evaluate the wettability of the PLA and PLA plasma modified samples. An equal volume of distilled water (100 μl) was placed on each dry sample by means of a micropipette, forming a drop on the surface. Photos were taken through lenses (LEITZ IIA optical stage microscope equipped with LEICA DFC320 video-camera) to record drop images. Measure of the contact angle was performed by analyzing drop images (3 for each samples) using Scion Image software for Windows.

2.7. Protein Adsorption Assay

Protein adsorption assays were performed in triplicate using FBS. PLA, PLA-COOH and PLA-NH_2 samples (1 cm^2) were covered with 200 μl of undiluted FBS and incubated for 24 h at 37 °C. At the end of incubation, serum was removed and films were washed three times in phosphate buffer (PBS, pH = 7.4). Adsorbed proteins were collected by incubating samples with 1 ml of 2% sodium dodecyl sulfate (SDS) solution in PBS for 24 h at room temperature and under vigorous shaking. Culture grade polystyrene (PS) dishes were used as control surface for protein binding. Amount of adsorbed proteins was measured in triplicate using a commercial protein quantification kit (Pierce, Rockford, IL, USA) based on bicinchoninic acid (BCA) colorimetric detection of the cuprous cation obtained by protein Cu^{2+} reduction in an alkaline medium. The sample optical density (O.D.) was read at 562 nm against a calibration curve using a bovine serum albumin (BSA), working range of 5–250 μg · ml^{-1}. The results were expressed as micrograms of total protein adsorbed for cm^2 ± standard deviation (S.D.). Patterns of

adsorbed proteins have been analyzed using SDS polyacrylamide gel electrophoresis (PAGE). Protein samples were denatured by boiling for 3 min, centrifuged at 12 000 *g*; and then a 10 μl volume was loaded onto a 10% separating polyacrylamide gel with a 4% stacking gel. Electrophoresis was conducted at 100 V by an electrophoresis system (BioRad Mini-Protean II, Milan, Italy). Proteins were stained by a BioRad Silver Stain Plus kit.

2.8. Cell Adhesion and Proliferation

Cell adhesion and proliferation onto PLA and plasma modified PLA samples was assessed using 3T3 mouse fibroblast (ATCC CCL-92), MC-3T3 E1 murine pre-osteoblasts (ATCC CCL-240),[25] and immortalized human keratinocytes (HaCaT),[26] grown in DMEM (3T3mouse fibroblast and HaCaT) or IMDM (MC-3T3 E1 mouse pre-osteoblasts) medium supplemented with 10% FBS, penicillin ($100\ U \cdot ml^{-1}$), streptomycin ($100\ mg \cdot ml^{-1}$), and L-glutamine (2 mM) (Euroclone, Milan, Italy) in a humidified atmosphere containing 5% CO_2 at 37 °C. Cell adhesion was assessed seeding 200 μl of cell suspension (5×10^5 cell $\cdot ml^{-1}$ in DMEM 10% FBS) onto PLA and plasma modified PLA samples (1 cm^2) for 4 h at 37 °C.

After incubation, unattached cells were removed by washing with fresh medium, while adherent cells were counted in ten different fields per sample at 10× magnification using an inverted microscope connected with a Leica DFC320 camera. Scoring was performed by three separate observers, blind to the PLA type observed, using Leika QWin software and expressed as total adherent cell number for $cm^2 \pm$ S.D. Adherent cells were incubated for further 48 h at 37 °C.

At the end of the incubation time, cell proliferation was assessed using Tox-8 assay. Briefly, a 10% solution of Alamar blue (resazurine, Sigma–Aldrich) was added to growth medium of various types of cells and incubated for 4 h at 37 °C. Medium samples (200 μl) were then analyzed in a fluorimeter (excitation wavelength = 560 nm, emission wavelength = 590 nm). The method is based on the dye resazurine oxydoreduction induced by cells and the O.D. for all samples was expressed as percentage of the O.D. values measured for control (PLA) samples ± S.D. At the end of the Tox-8 assay, cells were washed with PBS, fixed with an ice-cold 3% sucrose–3.7% formaldehyde solution for 30 min and stained with a solution of 1% acridine orange for 15 min in the dark. The metachromatic dye acridine orange excited by blue light (488 nm) emits a green fluorescence when bound to DNA and a red one when bound to single chain RNA. Samples were photographed through a Leica DM2500 fluorescence microscope. For each of PLA and PLA plasma treated samples ten photos were collected using a Leica DFC320 camera.

2.9. Statistical Analysis

Statistical analysis of data was performed using Graph Pad Prism 2.01 software using two-way Anova Test followed by Bonferroni's post hoc test method taking $p < 0.05$ as the minimum level of significance.

3. Results and Discussion

The plasma process described in this paper is used to modify the surface of biocompatible PLA films using DAP and AA to add, respectively, amino and carboxylic groups, at atmospheric pressure. A similar plasma deposition has been already proposed under high vacuum conditions.[19]

In plasma chemistry several different elementary reactions can occur simultaneously, therefore the choice of the process parameters is a key feature of the plasma treatment. In fact, in order to retain the monomer structure during direct plasma processing, the main parameters involved are low power input, high working pressures and short residence time of the molecule in the plasma. Yasuda[27] employed an external parameter called "Yasuda factor" to express the plasma energy density, defined as W/FM, where W is the power, F the flow rate, and M is the molecular weight: a smaller Yasuda factor correspond to less monomer fragmentation.[27] Another fundamental aspect to understand chemical mechanisms related to plasma polymerization is the analysis of the gas phase. The Optical Emission Spectra of AA (Figure 2A) and DAP (Figure 2B) glow discharge showed, in both cases, a relatively high hydrogen emission (peak at $666\ \lambda \cdot nm^{-1}$), indicating that the contribution to the initiation of the polymerization by the opening of double bonds in the case of AA is small according to Yasuda.[28]

According to these initiation mechanisms the overall polymer formation by glow discharge can be represented by the following reactions:

$$M_a - H \rightarrow M_a^{\bullet} + H^{\bullet} \quad \text{initiation}$$

$$M_b - H \rightarrow M_b^{\bullet} + H^{\bullet}$$

$$M_a^{\bullet} + M_b^{\bullet} \rightarrow (M_a - M_b) \quad \text{recombination}$$

$$(M_a - M_b) \rightarrow (M_a - M_b)^{\bullet} \quad \text{reinitiation}$$

where M indicate the monomer and a and b the number of repeating units.

The ATR spectra for PLA, PLA-COOH and PLA-NH_2 were reported in Figure 3. The ester groups (1 740 cm^{-1}) were present on the surface of all samples. The ATR spectrum for PLA-COOH samples showed the presence of OH groups (O–H stretching at 3 140 cm^{-1} and O–H bending at 1 405 cm^{-1}), with a signal at 1 620 cm^{-1} corresponding to the C=O stretching of AA due to its deposition/coating. PLA-NH_2 samples showed at 3 300 cm^{-1} N–H stretching and at 1 660 cm^{-1} amide N–H bending, indicating DAP coating onto the PLA surface.[29]

DOI: 10.1002/ppap.201100139

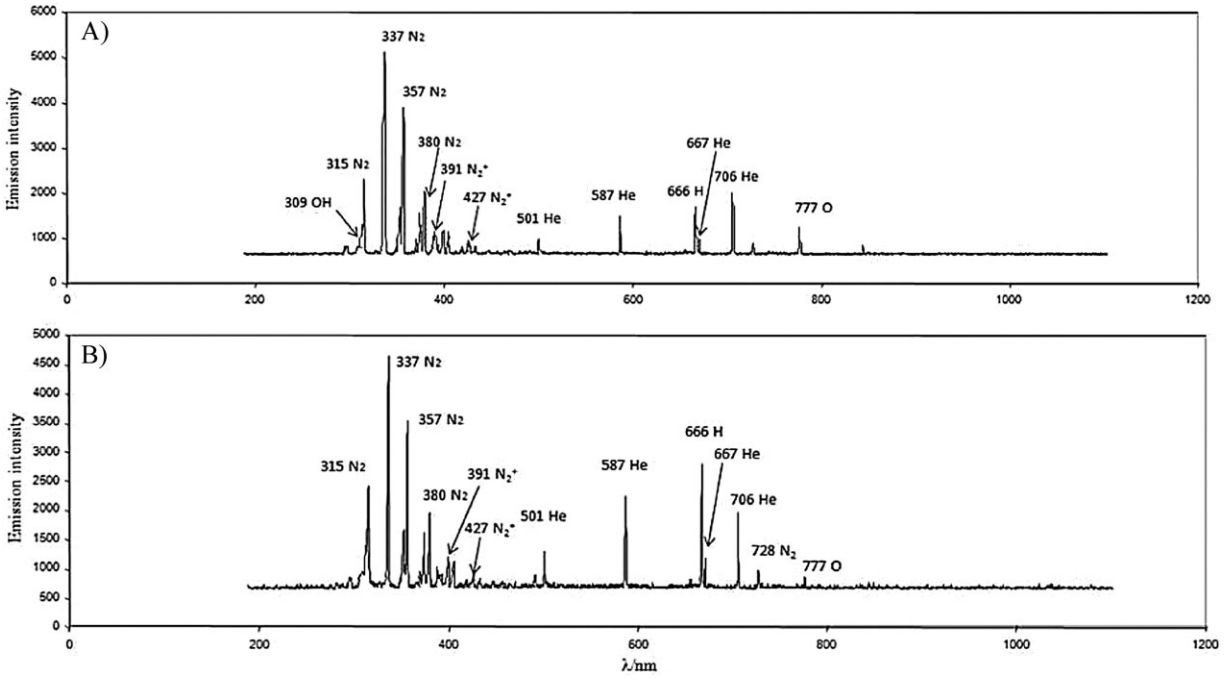

Figure 2. (A) Optical emission spectrum of a He/AA atmospheric plasma, 210 W, 90 s, 0.224 ml · min^{-1} of AA. Helium flux 3 l · min^{-1}. (B) Optical emission spectrum of a He/DAP atmospheric plasma, 1 000 W, 90 s, 0.322 ml · min^{-1} of DAP. Helium flux 3 l · min^{-1}.

Surface chemical modifications induced by plasma deposition were also characterized by XPS analyses. Table 1 showed the O/C and N/C ratios obtained from the quantification of XPS core peak areas for PLA films after helium, DAP, and AA coating under different processing conditions. In the first line, the O/C and N/C ratios of the untreated sample are reported for reference.

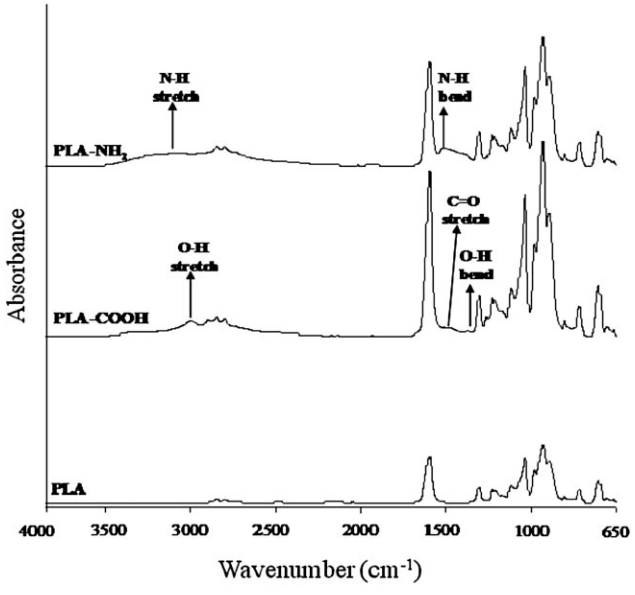

Figure 3. FTIR-ATR absorbance spectra to compare original PLA, PLA-COOH (treated with AA) and PLA-NH_2 (treated with DAP).

The XPS core lines of C1s, O1s and N1s were studied in detail for all the samples and their deconvolutions were shown in Figure 4, 5 and 6, respectively. The detailed assignment of the different components in terms of chemical states was listed in Table 2.

It has to be noted that a small tail is always present at the low binding energy side of the C1s and O1s peaks, which is an artifact due to the surface charging effect.

In Figure 4 the C1s line acquired on the untreated PLA film (PLA-ref, control sample) is shown and compared to that acquired on the treated samples (PLA-He, PLA-NH_2 and PLA-COOH).

In contrast to the theoretical 1:1:1 ratio of C−H (C1s#1, 285 eV)/C−O (C1s#2, 287.0 eV)/O−C=O (C1s#3, 289.1 eV) expected from literature for pure PLA, a higher peak at 285 eV appears in the reference sample, indicating an excess of hydrocarbons on untreated PLA surface. According to many authors, this may arise from PLA source material itself as well as from adsorption of adventitious hydrocarbons from the atmosphere.[30,31]

In Figure 5 the O1s peak of the reference and treated samples is shown. Regarding the untreated PLA surface, the O1s core line is dominated by the two components typical of the pure PLA: the C=O* oxygen (≈531.9 eV) and the OC−O* oxygen (≈533.4 eV). The asterisk denotes the atom the binding energy is associated to.

Finally, no signal was detected in the nitrogen region on the untreated PLA surface, as can be seen from Figure 6.

Table 1. Comparison between untreated and plasma treated PLA samples. PLA He describe the activation process preliminary at the deposition stage. PLA-NH_2 and PLA-COOH represent the deposition of ppDAP and ppAA films.

Sample	Carrier	*P* [bar]	[ml]	W_{RF} [W]	*d* [mm]	O/C	N/C
PLA ref	Untreated	–	–	–	–	0.47	–
PLA He activation	He	1.2	–	1 000	2.5	0.57	–
PLA-NH_2	He	1.2	0.322 DAP	1 000	2.5	0.74	0.21
PLA-COOH	He	1.2	0.224 AA	210	2.5	0.67	0.03

In order to summarize the modifications induced in the treated samples, an XPS core lines analysis was performed to highlight the chemical changes induced by the different coatings.

The plasma deposition, as before described, is composed of two stages: the first is the sample activation through the exposure of the surface to an helium discharge; the second is the coating with films containing functional groups (COOH-functional groups by plasma AA discharge or N-functional groups by plasma DAP discharge).

The effect of He activation pre-treatment is visible from XPS analyses. In fact, the C1s signal shows a slight decrease of the peak at 285 eV (C−C, C−H) and an increase of C−O and O−C=O signals at 287 and 289.1 eV, respectively. Besides, a small peak arises between the CH and CO components, around 286.5 eV. This peak is due to C−OH or C−O−C bounds due to polymer chain rearrangements during the He treatment.

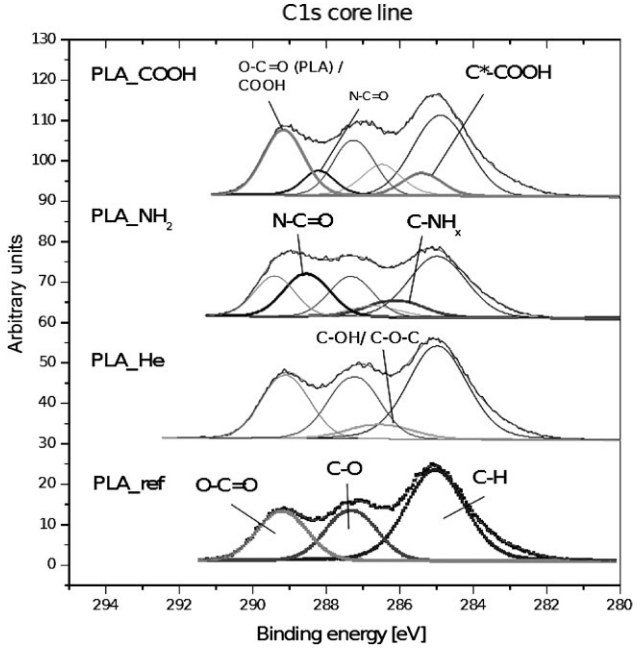

Figure 4. XPS spectra of the C1s region for the untreated (PLA_ref) sample and for the samples treated with He (PLA_He), DAP (PLA_NH_2), and AA (PLA_COOH) plasma discharge. The main effects of each specific treatment are highlighted with thicker lines and labeled with the correspondent functional group.

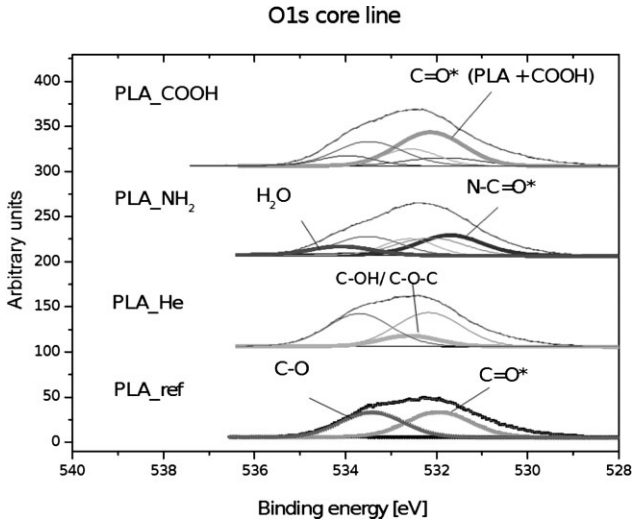

Figure 5. XPS spectra of the O1s region for the untreated (PLA_ref) sample and for the samples treated with He (PLA_He), DAP (PLA_NH_2), and AA (PLA_COOH) plasma discharge. The main effects of each specific treatment are highlighted with thicker lines and labeled with the correspondent functional group.

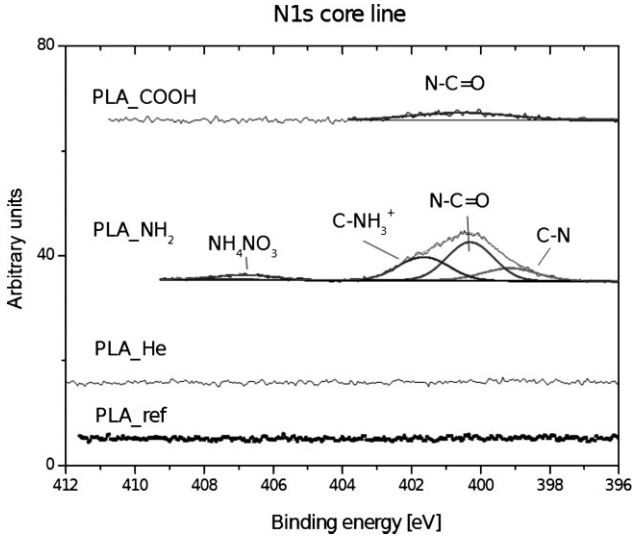

Figure 6. XPS spectra of the N1s region for the untreated (PLA_ref) sample and for the samples treated with He (PLA_He), DAP (PLA_NH_2), and AA (PLA_COOH) plasma discharge. The main effects of each specific treatment are highlighted with thicker lines and labeled with the correspondent functional group.

DOI: 10.1002/ppap.201100139

Table 2. Effect of different plasma treatments on XPS C1s, O1s and N1s core lines: deconvolution of the different lines, interpretation of the different components and relative binding energies.

	PLA ref	PLA_He	PLA_NH_2	PLA_COOH
C1s#1	C−H 285 eV	C−H	C−H	C−H
C1s#2	C−O 287.28 eV	C−OH/C−O−C 286.5 eV	C−N 286 eV	C*−COOH 285.4 eV
C1s#3	O−C=O 289.18 eV	C−O	C−OH/C−O−C	C−OH/C−O−C
C1s#4		O−C=O	C−O	C−O
C1s#5			N−C=O 288.5 eV	N−C=O
C1s#6			O−C=O	O−C=O/HO−C=O 289.17 eV
O1s#1	O−C=O* 531.92 eV	O−C=O*	N−C=O* 531.7 eV	N−C=O*
O1s#2	C−O 533.43 eV	C−OH/C−O−C 532.6 eV	O−C=O*	O−C=O*/HO−C=O* 532.06 eV
O1s#3		C−O	C−OH/C−O−C/NO_3	C−OH/C−O−C
O1s#4			C−O	C−O
O1s#5			H_2O	H_2O
N1s#1			C−N 399.1 eV	N−C=O
N1s#2			N−C=O 400.3 eV	
N1s#3			C − NH_3^+ 401.6 eV	
N1s#4			NH_4NO_3 406.7 eV	

A pure helium plasma does not contain any chemically reactive species and normally leads to radical formation, cross-linking, or double bond formation on polymer surfaces. In our sample it has been observed an increasing in oxygen content probably due both to oxygen and nitrogen impurities always present in the discharge gas and the presence of activated species on PLA surface that tend to react with oxygen when exposed to air.[32]

On the other hand the treatment with plasma polymerized DAP creates new chemical states on the PLA surface as can be seen from the deconvolution of C1s, O1s and N1s core lines.

The comparison between the C1s signal of PLA-ref and PLA-NH_2 samples (Figure 4), in fact, shows that plasma polymerization of DAP resulted in a strong decrease of the prominent hydrocarburic component at 285 eV and of the oxidized components associated with the PLA monomer (C−O, 287.3 eV and O−C=O, 289.2 eV). Moreover, two new peaks arise at 286 and 288.5 eV, attributed to amine (C−NH_x) and amide (N−C=O) species. This assignment is validated by the deconvolution of the O1s peak showed in Figure 5 and of the N1s core line in Figure 6.

In Figure 6 in particular we could observe that a prominent peak is visible in the nitrogen BE range (around 400 eV) in the PLA-NH_2 sample, demonstrating that nitrogen has been effectively grafted on the PLA surface where it is bound to carbon in amine (C−N, 399 eV) and amide (N−C=O, 400.3 eV) functional groups. Some contamination due to the precursor retention has also been revealed in the form of NH_4NO_3 composites (406.7 eV). The deconvolution of O1s peak on PLA-NH_2 samples (Figure 5) confirmed the presence of amide groups. In addition to the O−C=O, C−OH/C−O−C, and C−O components (at 532, 532.5 and 533.5 eV, respectively), in fact, attributable to the He-treated PLA, a prominent shoulder on the right side of the O1s peak appears, which we fitted with a component at 531.7 eV assigned to N−C=O groups. For sake of accuracy, a fifth component was placed on the high energy side of the peak, due to water molecules retention.

Regarding the effect of AA deposition on the PLA films, the presence of COOH groups is confirmed by XPS analyses. In the C1s core line (Figure 4) of sample PLA-COOH, in fact, it is evident the increase of the component placed at 289.1 eV, due to O−C=O bounds. This is associated to the rise of a new component at 285.4 eV which is due to the backbone carbon atom that is directly bonded to terminal carboxylic groups (C*-COOH).[33,34] Therefore, the above augmented component at 289.1 eV can be assigned to signal coming from both PLA O−C=O groups and from COOH groups grafted on the PLA surface. A small contamination of amide species was also present, due to nitrogen impurities in the discharge gas mixture.[35,36]

The deconvolution of O1s peak on PLA-COOH samples (Figure 5) confirmed the above description. We observe an augmented O−C=O* peak, which accounts for both the PLA O−C=O and for the COOH signals. The other peaks are: the C−OH/C−O−C and C−O components (532.5 and 533.5 eV, respectively) attributable to the He-treated PLA, a compo-

nent at 531.7 eV assigned to N–C=O groups and a fifth component on the high energy side due to water molecules retention (534 eV).

All the characterization analysis lead to conclude that AA, using low polymerization power, does not only break the double bond C=C (π bond), with consequent diradical formation as expected, but contributes to starting polymerization by the extraction of an hydrogen atom, as shown in OES spectra. Both ATR-FTIR and XPS analyses show as at low power there is a structure retention in deposited AA films (in particular carboxylic groups). Moreover, the absence of C=C double bonds connotes that a part of the double bonds are broken in the initiation process and the remaining part (the majority) broke during the film growing process by subsequent grafting of oligomeric units.

Using DAP as precursor results in a layer containing carbon (C), hydrogen (H) and nitrogen (N) with a chemical structure of reactive groups not well defined.

An explanation of the reaction mechanism is proposed in Figure 7. When working in controlled atmosphere (atmospheric pressure reaction chamber filled with nitrogen), it is possible to express two different hypothesis for the formation of a radical, either by extraction of an hydrogen atom from a primary/secondary carbon or by extraction of an hydrogen atom from amino functionality, or the formation of a diradical. Nevertheless the similar energy levels of both reaction channels suggest that both hypothesized mechanisms could occur simultaneously producing the coupling of radicals in oligomers to obtain the polymer. All the existing literature in this field describes depositions performed by using pure precursors. In this case the deposition has been performed using a 20% oxygen atmosphere (environmental air) allowing the contemporary film coating with aminic (from DAP) and both amidic and carboxylic functionalities (resulting of the oxygen recombination with α-amino methylene radicals from DAP), as shown in Figure 7. This experimental strategy has been adopted to compare protein adsorption, and both cell adhesion and proliferation properties of a pure PLA-COOH[16] with a mixed (PLA-NH_2/PLA-COOH) layer. The above described relations are complex and regulated by the hydrophilic/hydrophobic plasma modified surface constituents balance. These results highlight that plasma depositions could be widely used to generate different physical and chemical biomaterials outer molecular layer surface modifications, while retaining their bulk properties.[6]

For these reasons in addition to the above described chemical analysis, the ability of the proposed atmospheric

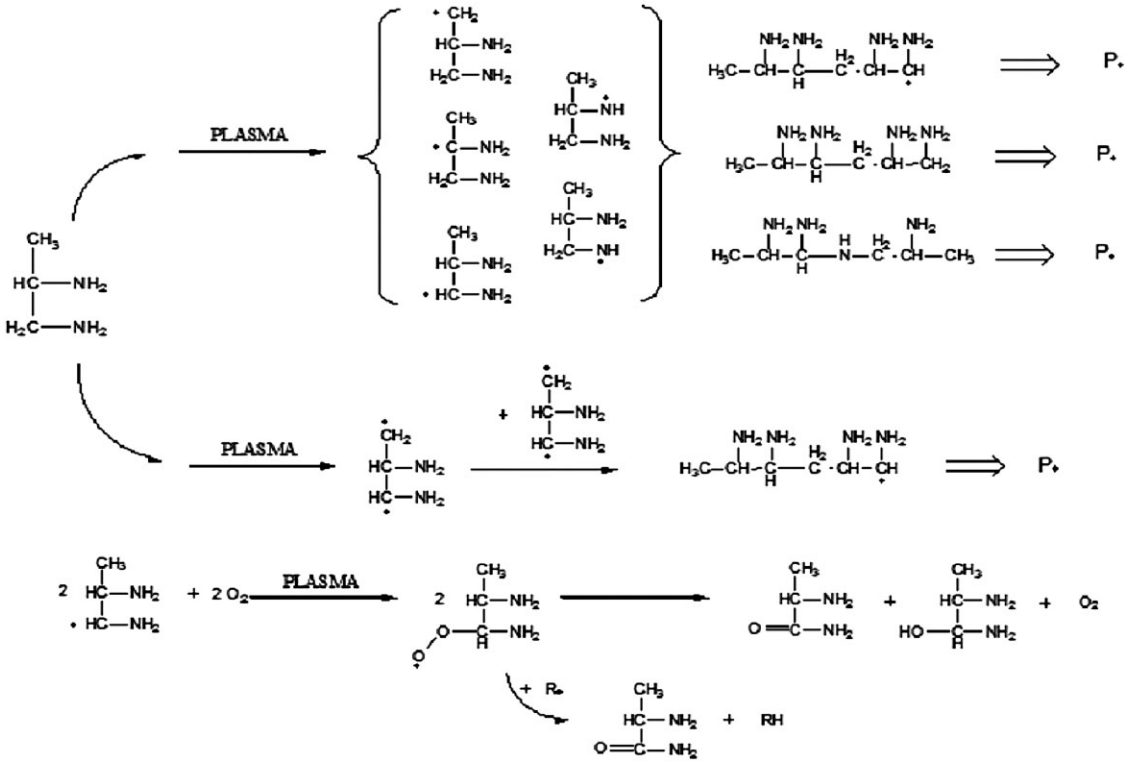

Figure 7. Proposed reaction mechanism of DAP. It is possible to observe the formation of a radical (either extraction of an hydrogen atom from a primary/secondary carbon or extraction of an hydrogen atom from aminic functionality) starting from DAP and the formation of a diradical. The final product is the coupling of the different radicals in diverse oligomers to obtain the polymer.

DOI: 10.1002/ppap.201100139

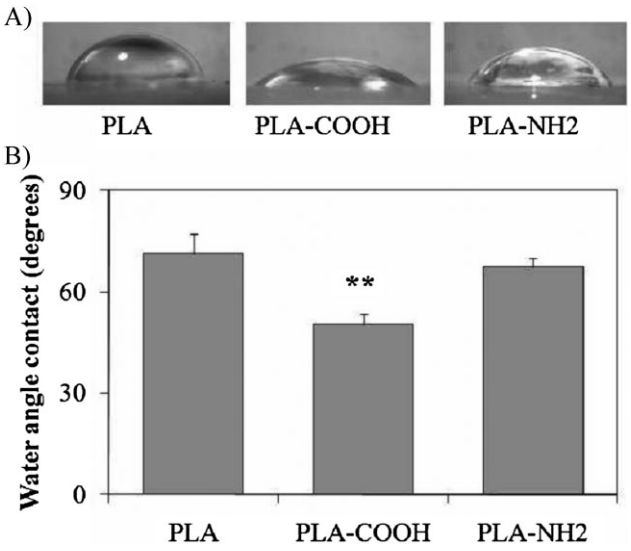

Figure 8. (A) Water drop profiles and (B) contact angle measurements (degrees ± S.D.) for normal PLA, PLA enriched with carboxylic (PLA-COOH), and aminic (PLA-NH_2) groups. ($^{**}p < 0.001$ compared to PLA).

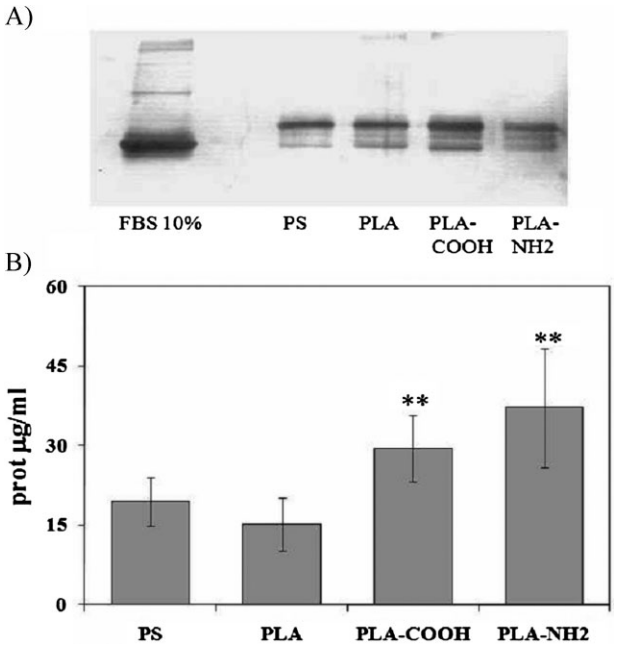

Figure 9. (A) Representative silver staining of protein adsorbed onto PLA, PLA-COOH and PLA-NH_2 separated onto a 10% SDS-PAGE gel. (B) BCA quantification of protein adsorbed onto control PS disks, PLA, PLA-COOH, and PLA-NH_2. $^{**}p < 0.001$, compared to control PLA.

pressure plasma deposition to alter PLA surface wettability has been investigated by the sessile water drop method. As a matter of fact, the first step in the mechanisms taking place at the interface between material and the surrounding environment is governed by the material surface energy and by the liquid environment surface tension. The adhesion work (W_a) is chosen as a thermodynamic parameter relevant for the adsorption characteristics of the surface, while it controls all physical interfacial events. W_a is calculated using the Dupré–Young equation

$$W_a = \gamma_1(1 + \cos\theta) \quad (1)$$

where θ is the contact angle and γ_1 is the surface tension of the liquid used for measurement (water). As shown in Figure 8A and B, the proposed atmospheric plasma depositions modify PLA wettability. In particular water static contact angle for normal PLA was $71.4^\circ \pm 6^\circ$, while the coating with AA as precursor (PLA-COOH) caused a dramatic increase in wettability ($50.3^\circ \pm 3.1^\circ$, $p < 0.001$ compared to PLA). On the contrary, coating with 1,2-diamminopropane as precursor (PLA-NH_2) did not change PLA wettability ($67.4^\circ \pm 2.5^\circ$).

The atmospheric pressure plasma modification described achieved an increase in polymer surface wettability mainly by the addition of carboxylic functional groups, as confirmed both by FTIR and XPS O1s core peak analysis. The observed increase in PLA-COOH surface wettability is mainly due to a better COOH functionalization efficiency. It is reasonable to speculate that the adhesion work extent increases with surface O/C.[36]

The existing relationship between polymer surface wettability and its ability to adsorb proteins from the surrounding biological environment is complex. In fact it is known that the effect of hydrophilic and hydrophobic balance of constituent chains on the polymer surface play a pivotal role in influencing protein adsorption. As atmospheric pressure plasma coatings modify PLA wettability, it is conceivable that it would also modify biomaterials' ability to adsorb proteins from FBS (Figure 9).

In fact, as is evidenced by 10% polyacrylamide gel stained with silver-staining (Figure 9A) PLA-COOH was able to adsorb an higher protein concentration compared to cell culture grade PS disks and normal PLA, while surprisingly also PLA-NH_2 increased the quantity of adsorbed protein. In particular, as indicated by the quantitative BCA test performed three times in triplicate, the untreated PLA adsorbed a serum protein concentration of $15.2 \pm 5\ \mu g \cdot ml^{-1}$, a protein amount not statistically different to that measured onto PS surface ($19.5 \pm 4.65\ \mu g \cdot ml^{-1}$), while PLA-COOH and PLA-NH_2 adsorbed, respectively, 29.5 ± 6.2 and $37.2 \pm 11.2\ \mu g \cdot ml^{-1}$ ($p < 0.001$ compared to PLA) (Figure 9B).

The existing literature data about the wettability and protein adsorption relationship are conflicting. Starting from the above described results we can speculate that the increased protein adsorption observed after atmospheric pressure plasma deposition, which not correlate with

wettability results, could be due to the different nature of the proteins interacting with the differently charged surfaces. The observed results for the more hydrophilic PLA-COOH surface could be explained by a major binding of serum hydrophilic proteins to the deposited COOH functionalities compared to what observed onto unmodified PLA and control PS. On the other hand the observed increase in protein adsorption onto the less hydrophilic PLA-NH_2 (less surface density of $-NH_2$ groups) surface is supposed to be due to the predominant binding of serum hydrophobic components by electrostatic interactions.

It is known that cell growth onto an artificial polymer is mainly determined by both its physical (i.e., surface wettability) and chemical (i.e., functional groups grafting) characteristics, either affecting surface protein adsorption and ultimately cell adhesion and spreading. As PLA scaffolds do not have natural cell binding sites, cellular attachment to such substrates is mainly modulated by the interactions between cell surface receptors (i.e., integrins) or cell membrane glycoproteins to serum protein, always present in the growth medium, not specifically adsorbed onto biomaterials surface during the incubation period.[37]

In order to evaluate the bioactivity and biocompatibiliy of the atmospheric pressure plasma modified PLA films, and eventually their effect on different cell types, the behavior of three different cell lines (murine fibroblasts and pre-osteoblasts and human keratinocytes) has been evaluated.

As shown in Figure 10 murine fibroblasts (3T3), murine pre-osteoblasts (MC-3T3), and human keratinocyte (HaCaT) were able to adhere onto PLA and plasma modified PLA, but MC-3T3 showed a higher affinity for PLA compared to the other cell types and this affinity was even higher onto PLA-COOH were pre-osteoblast spreaded, while this effect was less important onto PLA-NH_2. Cell scoring after 4 h adhesion confirmed these observations as MC-3T3 cells were present at a density of $23\,200 \pm 3\,600$ cell $\cdot$ cm^{-2} onto PLA while their number increased significantly onto PLA-COOH ($52\,400 \pm 4\,500$ cell $\cdot$ cm^{-2}) and PLA-NH_2 ($32\,200 \pm 6\,700$ cell $\cdot$ cm^{-2}), while HaCaT cells were $12\,000 \pm 1\,000$ cell $\cdot$ cm^{-2} onto PLA and $34\,500 \pm 1\,800$ cell $\cdot$ cm^{-2} and $26\,800 \pm 900$ cell $\cdot$ cm^{-2} onto PLA-COOH and PLA-NH_2, respectively.

On the contrary murine fibroblast showed a low affinity with all kind of PLA samples.

In fact, after 4 h of adhesion fibroblasts present onto PLA were $12\,000 \pm 3\,000$ cell $\cdot$ cm^{-2}, while cells scored onto PLA-COOH and PLA-NH_2 were $16\,000 \pm 800$ cells $\cdot$ cm^{-2} and 9000 ± 500 cells $\cdot$ cm^{-2}, respectively (Figure 11).

After 48 h, proliferation of adherent cells was assessed both observing cells stained with acridine orange and using the TOX-8 assay that scores cell number as a measure of mitochondrial activity as observed by the modification of resazurine dye O.D. In Figure 12 it was quite evident a good cell proliferation for both MC-3T3 and HaCaT cells that

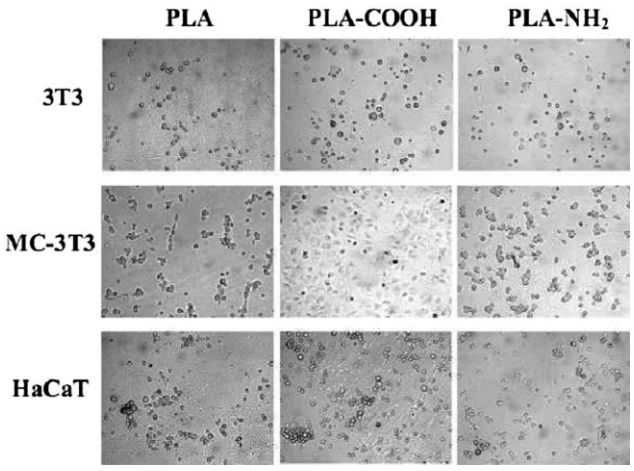

Figure 10. Cell morphology of fibroblast 3T3, pre-osteoblast MC-3T3 and HaCaT cells adherent to normal PLA, PLA-COOH, and PLA-NH_2 after 4 h incubation. Magnification = 10×.

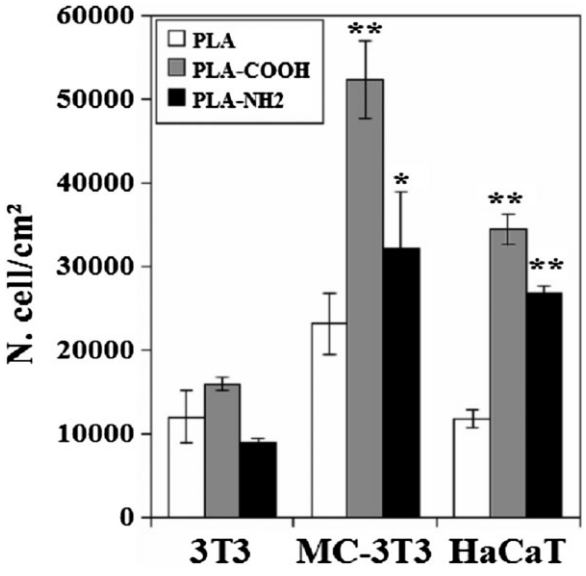

Figure 11. Cellular count of adherent fibroblast 3T3, pre-osteoblast MC-3T3, and HaCaT cells scored onto normal PLA, PLA-COOH and PLA-NH_2 after 4 h incubation. Adherent cells score was expressed as cell number $\cdot$ $cm^{-2} \pm$ S.D. $^{*}p < 0.05$; $^{**}p < 0.001$, compared to control PLA.

showed also a lightly red cytoplasm indicating the presence of a good metabolic activity (RNA presence). Moreover, HaCaT cells formed an almost confluent cell layer onto PLA-COOH. As expected 3T3 fibroblast proliferated very slowly onto each surface. In Figure 13 the Tox-8 assay results were expressed as percentage of O.D. measured onto PLA samples in order to normalize the differences observed in the control samples. These data indicated that plasma deposition for producing PLA-COOH samples was the most effective in promoting cell proliferation especially for MC-3T3

DOI: 10.1002/ppap.201100139

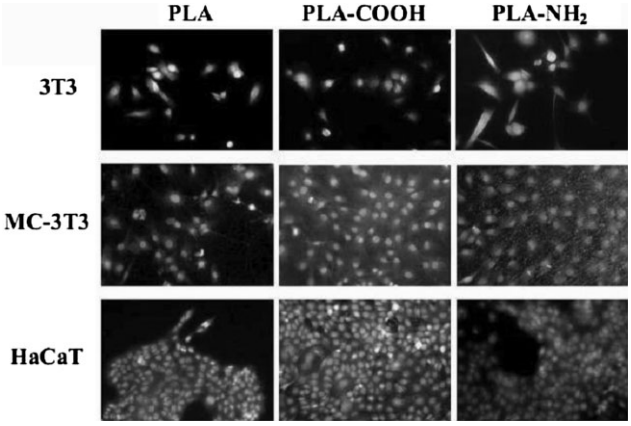

Figure 12. Cell morphology of fibroblast 3T3, pre-osteoblast MC-3T3 and HaCaT cells after 48 h from seeding onto normal PLA, PLA-COOH, and PLA-NH_2. Cells were fixed with 3% sucrose–3.7% formaldehyde solution and stained with Acridine orange. Magnification = 10×.

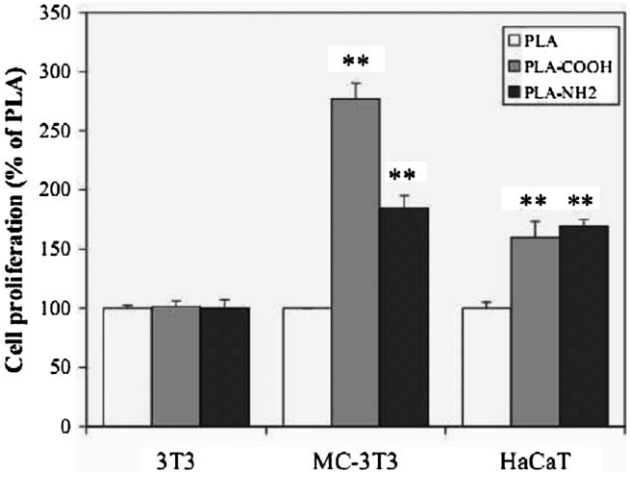

Figure 13. Tox-8 assay for cell proliferation. The O.D. for all samples was expressed as percentage of the O.D. values measured for control (PLA) samples ± S.D. $^{**}p < 0.001$ compared to control PLA.

osteoblast. Comparing Figure 11 and 13, it was also clear that surfaces promoting cell adhesion were also effective in supporting cell growth.

The PLA-COOH effects on cellular behavior has been already reported as acid termined surface promote cell adhesion and proliferation.[38] It is also noteworthy that PLA-NH_2, whose wettability was not changed, was able to bind an higher protein concentration compared to PLA and to stimulate cell adhesion and proliferation even if at a lower degree compared to PLA-COOH.

This NH_2 effect has been already documented for hydrogels functionalized with primary amine for the proliferation of keratinocyte[39,40] and chitosan films acetylated for neurite outgrowth.[41]

The MC3T3 pre-osteoblast cells grow faster onto PLA-COOH than onto untreated PLA, according to the observations performed onto plasma modified hydrophilic surfaces.[42] Nevertheless MC3T3 were able to proliferate, even if at a lower extent, also onto the hydrophobic surface of PLA-NH_2 similarly to rat calvaria osteoblasts onto plasma modified hydrophobic polytetrafluoroethylene (PTFE).[43]

Finally murine fibroblasts 3T3 seem to be unaffected by the presence of COOH and NH_2 groups onto the PLA surface as no changes were observed in their cell adhesion and proliferation in presence of 10% FBS. A similar behavior has been already observed onto AA coated surfaces, both in presence and absence of serum.[44]

4. Conclusion

This experimental approach allowed to compare the biological effects of a pure COOH with those induced by a mix of NH_2, CONH, and COOH functionalities, obtained by plasma deposition onto P(D,L)LA at atmospheric pressure. Our results show that the described atmospheric pressure plasma deposition is able to effectively improve the P(D,L)LA biocompatibility and bioactivity toward osteoblasts and keratinocytes. These results have been achieved through a modulable addition of coatings containing COOH and NH_2 groups onto polymer surface using atmospheric plasma deposition that allows an high efficiency conjugated with low process costs, as this method is characterized by the absence of large vacuum devices and could be immediately transferred to line production. The proposed method could foster the use of plasma deposition in skin and bone tissue engineering.

Acknowledgements: Authors thanks Dr. E. Ciancio from the Plasma Technology Observatory of Environment Park, for the precious technical help. This work was supported by University of Eastern Piedmont "A. Avogadro" local funds (60% Dept. Fund 2009) and from Environment Park S.p.A.

Received: July 11, 2011; Revised: November 9, 2011; Accepted: December 19, 2011; DOI: 10.1002/ppap.201100139

Keywords: atmospheric pressure plasma deposition; cell adhesion; cell proliferation; osteoblast; polylactic acid

[1] A. G. Andreopoulos, E. Hatzi, M. Doxastakis, *J. Mater. Sci.: Mater. Med.* **1999**, *10*, 29.
[2] R. E. Drumright, P. R. Gruber, D. E. Henton, *Adv. Mater.* **2000**, *12*, 1814.
[3] C. M. Agrawal, J. Best, J. D. Heckman, B. D. Boyan, *Biomaterials* **1995**, *16*, 1255.
[4] J. Slager, A. J. Domb, *Adv. Drug Delivery Rev.* **2003**, *55*, 549.

[5] R. Morent, N. De Geyter, M. Trentesaux, L. Gengembre, P. Dubruel, C. Leys, E. Payen, *Plasma Chem. Plasma Process.* **2010**, *30*, 525.
[6] C. Oehr, *Nucl. Instrum. Methods Phys. Res., Sect. B* **2003**, *208*, 40.
[7] P. K. Chu, J. Y. Chen, L. P. Wang, N. Huang, *Mater. Sci. Eng.* **2002**, *36*, 143.
[8] J. M. Morais, F. Papadimitrakopoulos, D. J. Burgess, *AAPS J.* **2010**, *12*, 188.
[9] B. D. Ratner, *J. Mol. Recognit.* **1996**, *9*, 617.
[10] R. Förch, Z. Zhang, W. Knoll, *Plasma Process. Polym.* **2005**, *2*, 351.
[11] J. A. Neff, P. A. Tresco, K. D. Caldwell, *Biomaterials* **1999**, *20*, 2377.
[12] R. Hansen, J. Pascale, *J. Polym. Sci., Part A* **1965**, *3*, 2205.
[13] D. T. Clark, *J. Polym. Sci.: Polym. Chem. Ed.* **1978**, *16*, 911.
[14] S. O'Kell, T. Henshaw, G. Farrow, C. Jones, *Surf. Interface Anal.* **1995**, *23*, 319.
[15] S. Pringle, V. Joss, C. Jones, *Surf. Interface Anal.* **1996**, *24*, 1.
[16] L. Detomaso, R. Gristina, G. S. Senesi, R. d'Agostino, P. Favia, *Biomaterials* **2005**, *26*, 3831.
[17] C. Oehr, M. Müller, B. Elkin, D. Hegemann, U. Vohrer, *Surf. Coat. Technol.* **1999**, *25*, 116.
[18] Z. Ma, C. Gao, Y. Gong, J. Shen, *Biomaterials* **2003**, *24*, 3725.
[19] D. B. Haddow, S. McNeil, R. D. Short, *Plasma Process. Polym.* **2006**, *3*, 419.
[20] A. D. Hanson, M. Wall, B. Pourdeyhimi, E. G. Loboa, *J. Biomater. Sci., Polym. Ed.* **2007**, *18*, 1387.
[21] C. M. Alves, Y. Yang, D. L. Carnes, J. L. Ong, V. L. Sylvia, D. D. Dean, C. M. Agrawal, R. L. Reis, *Biomaterials* **2007**, *28*, 307.
[22] J. L. Polan, B. Morse, S. Wetherold, R. E. Villanueva-Vedia, C. Phelix, E. Barera-Roderiquiz, D. Waggoner, N. Goswami, O. Munoz, C. M. Agrawal, S. R. Bailey, *Cardiovasc. Radiat. Med.* **2002**, *3*, 176.
[23] J. H. Lee, G. Khang, J. W. Lee, H. B. Lee, *J. Colloid Interface Sci.* **1998**, *205*, 323.
[24] www.grinp.com.
[25] F. Renò, V. Aina, S. Gatti, M. Cannas, *Biomaterials* **2005**, *26*, 5594.
[26] P. Boukamp, R. T. Petrussevska, D. Breitkreutz, J. Hornung, A. Markham, N. E. Fusenig, *J. Cell Biol.* **1988**, *106*, 761.
[27] H. Yasuda, Ed., *Plasma Polymerization*, Academic Press Inc., Orlando, FL **1985**.
[28] H. Yasuda, *J. Macromol. Sci., Chem.* **1976**, *A10*, 383.
[29] G. Socrates, Ed., *Infrared and Raman Characteristic Group Frequencies*, 3rd edition, J. Wiley and Sons Ltd., West Sussex, England **2001**.
[30] X. J. Dai, J. du Plessis, I. L. Kyratzis, G. Maurolev, M. G. Huson, C. Coombs, *Plasma Process. Polym.* **2009**, *6*, 490.
[31] R. Morent, N. De Geyter, T. Desmet, P. Dubruel, C. Leys, *Plasma Process. Polym.* **2011**, *8*, 171.
[32] T. R. Gengenbach, H. J. Griesser, *J. Polym. Sci., Part A: Polym. Chem.* **1999**, *27*, 2191.
[33] G. P. Lopez, D. G. Castner, B. D. Ratner, *Surf. Interface Anal.* **1991**, *17*, 267.
[34] G. Beamson, H. Briggs, Eds., *High Resolution XPS of Organic Polymers: The Scienta ESCA300 Database*, Wiley, New York **1992**.
[35] E. Kiss, I. Bertoti, E. I. Vargha-Butler, *J. Colloid Interface Sci.* **2002**, *245*, 91.
[36] R. Daw, S. Candan, A. J. Beck, A. J. Devlin, I. M. Brook, S. MacNeil, R. A. Dawson, R. D. Short, *Biomaterials* **1998**, *19*, 1717.
[37] A. V. Janorkar, E. W. Fritz, K. J. L. Burg, A. T. Metters, D. E. Hirt, *J. Biomed. Mater. Res., Part B: Appl. Biomater.* **2007**, *81B*, 142.
[38] T. Sun, M. Higham, C. Layton, J. Haycock, R. Short, S. MacNeil, *Wound Repair Regen.* **2004**, *12*, 626.
[39] S. Rimmer, C. Johnson, B. Zhao, J. Collier, L. Gilmore, S. Sabnis, P. Wyman, C. Sammon, N. J. Fullwood, S. MacNeil, *Biomaterials* **2007**, *28*, 5319.
[40] C. Chatelet, O. Damour, A. Domard, *Biomaterials* **2001**, *22*, 261.
[41] T. Freira, H. S. Koha, K. Kazaziana, M. S. Shoichet, *Biomaterials* **2005**, *26*, 5872.
[42] M. Nakagawa, F. Teraoka, S. Fujimoto, Y. Hamada, H. Kibayashi, J. Takahashi, *J. Biomed. Mater. Res., A* **2006**, *7*, 112.
[43] H. Wang, D. T. K. Kwok, W. Wang, Z. Wu, L. Tong, Y. Zhang, P. K. Chu, *Biomaterials* **2010**, *31*, 413.
[44] M. Notara, N. A. Bullet, P. Deshpande, D. B. Haddow, S. MacNeil, J. T. Daniels, *J. Mater. Sci: Mater. Med.* **2007**, *18*, 329.

DOI: 10.1002/ppap.201100139